JOURNAL OF MATERIALS SCIENCE 27 (1992) 3599–3604

Hot-press sintering studies of amorphous silicon nitride powders

G. T. BURNS
Dow Corning Corporation, Midland, MI 48686-0995, USA
J. A. EWALD, K. MUKHERJEE
Department of Metallurgy, Mechanics and Materials Science, Michigan State University, East Lansing, MI 48824, USA

The hot-press sintering behaviour of amorphous Si_3N_4 powders prepared from the ammonia pyrolysis of polycarbosilane or hydridopolysilazane polymers was studied. In the presence of yttria and alumina, the amorphous powders sintered to $> 98\%$ of theoretical density at 2023 K. Both the microstructure and average four-point MOR bend strengths, of test bars machined from the sintered compacts were comparable to those obtained from UBE SN-E-10 Si_3N_4 powder processed under the same conditions. However, in contrast to commercial crystalline powders, between approximately 1690 and 1700 K the amorphous Si_3N_4 powders underwent a rapid shrinkage corresponding to 50–60% of the total densification. In this narrow temperature regime, a radical change in morphology and phase composition of the amorphous powder occurred. Prior to 1690 K, the Si_3N_4 powders were totally amorphous as determined by X-ray diffraction analysis and consisted of angular shards with an average particle size of 2–3 μm. Samples quickly cooled after heating to 1700 K, consisted of a 53/47 mixture of equiaxed α and β Si_3N_4 crystallites with an average particle size of 0.1–0.3 μm. Thus, the rapid densification at ~1700 K is identified with the amorphous to (α + β) transition. Beyond ~1700 K, these samples gradually densified to the maximum density as mentioned. The fully densified samples consisted of 100% β-Si_3N_4 phase.

1. Introduction

Because of its corrosion, oxidation, and thermal-stress resistance and its high-temperature strength retention, silicon nitride has emerged as one of the leading candidates for high-temperature structural applications [1]. To date, the sintering of crystalline silicon nitride powders requires the use of additives to create a high-temperature liquid phase through which mass diffusion and consolidation occur. Unfortunately, the presence of this glassy phase inevitably deteriorates the high-temperature properties for which sintered silicon nitride is sought after. As a result, many workers have investigated the production and sintering characteristics of amorphous silicon nitride powders with the intention of minimizing the amount of additives required to sinter the powders. Amorphous silicon nitride powders are available from: (i) the thermal decomposition of $Si(NH)_2$ [2–4]; (ii) the gas-phase reaction of silane and ammonia between 773 and 1173 K [5]; (iii) the reaction of $SiCl_4$ with ammonia in a thermal plasma [6–8]; (iv) the CO_2 laser-induced decomposition of silane and ammonia [9, 10]; and (v) the thermal decomposition of cross-linked preceramic polymers in ammonia atmospheres [11]. To date, several of the powders have been successfully densified with the addition of sintering additives such as Mg_3N_2 [3] and mixtures of Y_2O_3 and Al_2O_3 [10, 12]. However, attempts to sinter amorphous powders without the addition of additives have been unsuccessful, despite the use of high pressures [13] and rapid heating rates [8].

This paper describes the sintering behaviour of amorphous silicon nitride powders prepared from the thermal decomposition of pre-ceramic polymers in ammonia atmospheres in the presence of Y_2O_3 and Al_2O_3 sintering aids.

2. Experimental procedure

All weighings and transfers were carried out in inert atmospheres. The polycarbosilane- [14] and hydridopolysilazane- [15] derived amorphous Si_3N_4 powders were prepared according to published procedures [11]. The crude powders were milled by using a Szeguari attritor mill in certified toluene with 6 mm Si_3N_4 milling media until an average particle size of 1–3 μm was obtained. Particle size was analysed by using a Microtrac Particle Size Analyzer. After collecting and drying the comminuted, amorphous powders, 5 wt % of Y_2O_3 and 3 wt % of Al_2O_3 were added and the mixture attritor-milled (as above) for 1 h. The slurry was collected, dried and sieved through a

0022–2461

150 μm stainless steel sieve. All sintering studies were done on 10–12 g aliquots of the amorphous Si_3N_4 powders, with or without sintering aids, at a pressure of 27.6 MPa in a hot press (Model 3660-40T; Vacuum Industries) equipped with a 0.394-cm graphite die and punch set. The samples were fired at a rate of 10 K min^{-1} to the final temperature with a 30 min hold at 1473 K in a nitrogen atmosphere.

Bulk densities were measured according to ASTM C 373-72. Specific gravities were measured by helium pycnometry (Model MPY-2; Quantachrome Corp.). Four-point bend strengths were obtained on 1.5 × 2.0 × 25.0-mm test bars machined according to Milling Standard 1942 (MR). Iron, aluminium, calcium and oxygen analyses were done by Galbraith Laboratories. X-ray diffraction (XRD) of the powders was conducted using CuK_α radiation, 30 kV/15 mA, and scanning from $2\theta = 20°$ to 130°. The ratio of α to β-Si_3N_4 was determined by comparing the various peak heights and then normalizing to obtain the weight percent of each. Concurrent differential thermal/thermogravimetric analyses (DTA/TGA) were done on a Netzch instrument using a temperature ramp of room temperature to 1373 K at 20 K min^{-1} and 1373–1723 K at 10 K min^{-1}. A platinum crucible lined with tungsten foil was used as the sample holder.

Etching of polished surfaces was done with a mixture of 10 wt % NH_4F in 30% HF at ~353 K. Etching times ranged from 1–5 min.

3. Results and discussion

3.1. Preparation and characterization of amorphous silicon nitride powders

Amorphous silicon nitride powders were prepared from polycarbosilane (PCS) and hydridopolysilazane (HPZ) according to the procedure of Burns and Chandra [11]. The crude powders were reduced to an average particle size of 1.6 and 2.1 μm, respectively, by wet milling in toluene with silicon nitride milling media. The morphology of the comminuted amorphous powders is shown in Fig. 1. In general, the particles retained the overall shape and topography of the as-fired powders.

After milling, both sets of powders were analysed for their surface area, specific gravity and aluminium, iron, calcium and oxygen content. The results are summarized and compared against commercial Si_3N_4 powders in Table I. In general, the results for the two amorphous powders were quite similar and in terms of trace metal and oxygen content, the amorphous powders compared favourably with values reported in the literature for several commercial Si_3N_4 powders [7]. However, the Brunauer–Emmett–Teller (BET) surface

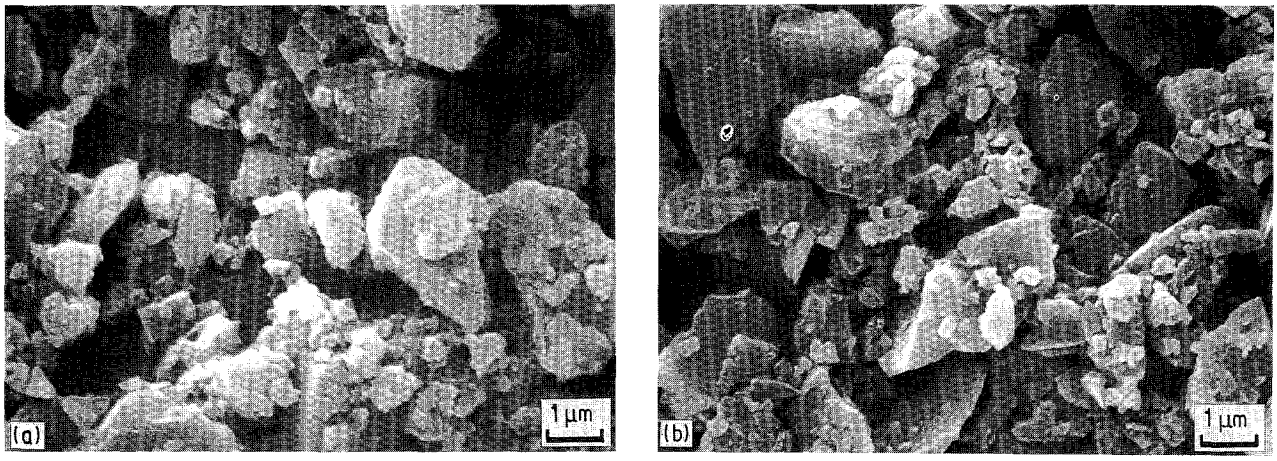

Figure 1 Morphology of comminuted, amorphous silicon nitride powders after attritor milling. Prepared from (a) PCS; (b) HPZ.

TABLE I Characterization of amorphous silicon nitride powders and comparison with commercial powders

Source	Surface area ($m^2 g^{-1}$)	Particle size (μm)	Specific gravity ($g cm^{-3}$)	Analysis of 1473-K powders				XRD data	
				Al	Fe	Ca	O_2 (wt%)	α (%)	β (%)
HPZ-673	284 ± 8	2.1	2.54	110	47	17	0.26	Amorphous	
PCS-823	276 ± 8	1.6	2.45	149	90	57	0.33	Amorphous	
UBE SN-E-10	16 ± 2	0.1–0.3	3.24	< 50[a]	< 100[a]	< 50[a]	0.06	95	5
Toyosoda[b]	12	<0.6	–	< 20	22	< 10	1.6	89	11
Starck[b]	15	0.5	–	600	400	300	1.4	95	5
Shinetsu[b]	–	–	–	1500	200	130	1.5	93	7
Toshiba[b]	–	–	–	20	70	70	1.5	–	

[a] Literature value reported by UBE.
[b] Values taken from 7.

area of both amorphous powders was very high, 276 ± 8 and $284 \pm 8\ m^2\ g^{-1}$ for the PCS- and HPZ-derived Si_3N_4 powders, respectively. Similar values for the surface area were obtained for the amorphous powders before comminution, and hence are a consequence of the powder synthesis and not the comminution step. In comparison, all commercial crystalline Si_3N_4 powders and most amorphous powders have surface areas of only 10–40 $m^2\ g^{-1}$ despite having a substantially smaller particle size. In fact, the only other abnormally high surface area, 183 $m^2\ g^{-1}$, was reported by Yamada, Kawahito and Iwai [4] for an amorphous powder prepared from the thermal decomposition of $Si(NH)_2$ in a NH_3 stream at 1273 K.

3.2. Sintering studies

In the absence of sintering aids, no densification of the HPZ-derived amorphous Si_3N_4 powder was observed under hot pressing conditions. Compacts fired to 2023 K with 27.6 MPa pressure were weak and easily fractured. Examination of a fracture surface under a scanning electron microscope (SEM) showed regions of localized grain growth or interparticle bonding but no macroscopic sintering. By XRD analysis, the compact consisted of 83% α- and 17% β-silicon nitride. However, under the same hot-press conditions and in the presence of 5 wt % Y_2O_3 and 3 wt % Al_2O_3, the HPZ powder sintered to $> 98.5\%$ of theoretical density. The resultant sintered compacts were 100% β-Si_3N_4.

A series of hot-press runs were made with the UBE-SN-E10, PCS and HPZ Si_3N_4 powders in which the final temperature and hold time were varied. None of the runs were optimized. After measuring their bulk density, the hot-pressed samples were machined into test bars according to Milling Standard 1942 (MR). Selected samples were further analysed by XRD and SEM analysis of both polished and etched surfaces. The results of the density, XRD and four-point MOR measurements are summarized in Table II. In general, the room temperature mechanical properties of dense Si_3N_4 are controlled by two microstructural parameters: the elongated β-grains, which can be characterized by the average aspect ratio; and the overall grain size [1]. Hence samples of dense Si_3N_4 with similar microstructures should have comparable mechanical properties. The microstructure of each amorphous powder and the UBE SN-E-10 powder hot-pressed to 2023 K (27.6 MPa pressure, 90 min hold at temperature) is shown in Fig. 2. In each case, the only crystalline phase observed by XRD was β-Si_3N_4. The SEM micrographs were taken on polished surfaces etched with a mixture of NH_4F and HF. Examination of the micrographs shows that both the size and the aspect ratio of the β-Si_3N_4 crystallites are equivalent in each sample. Thus the samples should have comparable mechanical properties. This is the case. Although the average four-point MOR was in the range 655–750 MPa, there is no statistical difference in the three means.

During each hot-press run, the degree of sintering was followed by the linear variable differential transformer (LVDT) output. In effect, the LVDT measures the movement of the pressure transferring ram and hence the density of the sample. A comparison of the LVDT curves for the HPZ-derived amorphous Si_3N_4 and UBE SN-E-10 powders, fired to 2023 K at a rate of 10 K min^{-1} with a pressure of 27.6 MPa, is shown in Fig. 3. The LVDT curve for the UBE SN-E-10 powder shows a typical, elongated 'S' curve. The UBE powder gradually densified with increasing temperature; the process began at 1600 K and continued until the temperature reached 1973 K. In contrast, under the same conditions, no densification of the HPZ-derived powder was seen until a temperature of ~ 1773 K was reached. At this point, the sample underwent a very rapid shrinkage corresponding to

TABLE II Comparison of amorphous Si_3Ni_4 powders with UBE SN-E-10

Si_3N_4 source	Sintering aids (wt %)	Final temperature (K)	Hold time (h)	Bulk density[a] ($g\ cm^{-3}$)	Four-point MOR (MPa)	XRD data α (%)	β (%)
HPZ	None	2023	1.5	1.19	–	83	17
	Y_2O_3 (5)/Al_2O_3 (3)	2023	1.5	3.23	655 ± 75.2 ($n = 6$)	0	100
	Y_2O_3 (5)/Al_2O_3 (3)	1973	1.5	3.23	714 ± 70 ($n = 4$)	–	–
	Y_2O_3 (5)/Al_2O_3 (3)	1823	3.0	3.18	474 ± 39 ($n = 4$)	16	84
PCS	Y_2O_3 (5)/Al_2O_3 (3)	2023	1.5	3.23	685 ± 61 ($n = 7$)	0	100
	Y_2O_3 (5)/Al_2O_3 (3)	1973	1.5	3.24	510 ± 156 ($n = 4$)	–	–
UBE SN-E-10	Y_2O_3 (5)/Al_2O_3 (3)	2023	1.5	3.23	750 ± 143 ($n = 6$)	0	100
	Y_2O_3 (5)/Al_2O_3 (3)	1973	1.5	3.22	714 ± 70 ($n = 4$)	–	–
	Y_2O_3 (5)/Al_2O_3 (3)	1823	3.0	3.22	693 ± 99 ($n = 4$)	55	46

[a] Theoretical bulk density = 3.27 $g\ cm^{-3}$.

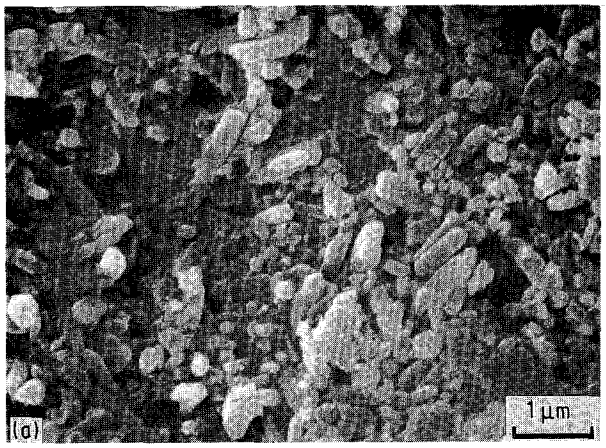

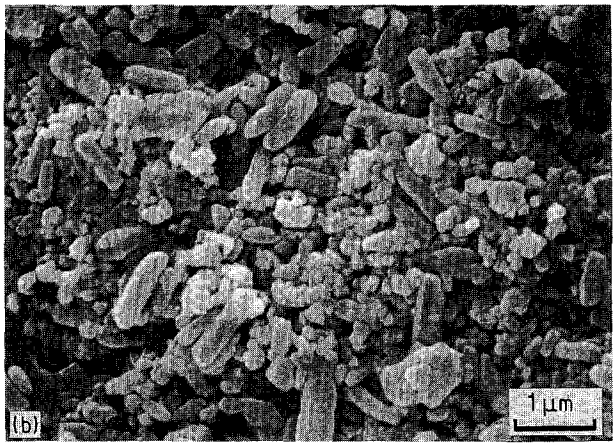

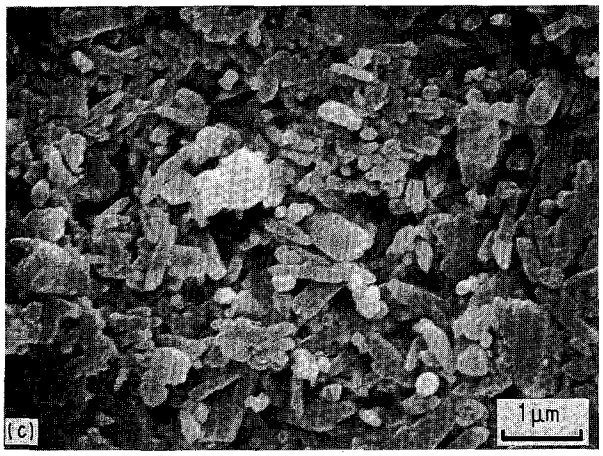

Figure 2 Comparison of the etched microstructure of sintered silicon nitride prepared from both amorphous silicon nitride powders and UBE SN-E-10. Micrographs are on polished surfaces etched with HF/NH_4F. Prepared from (a) PCS; (b) HPZ; (c) UBE SN-E-10. Note the similarity in the crystallite size.

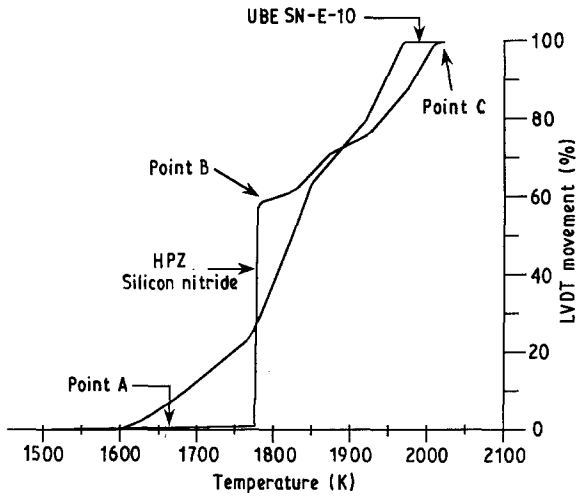

Figure 3 Comparison of LVDT curves for HPZ-derived amorphous silicon nitride and UBE SN-E-10 during hot pressing. Samples were heated at a constant 10 K min^{-1}.

approximately 60% of the total ram movement. The shrinkage occurred within a narrow (< 10 K) temperature band. To check for any thermal lag in the system and to see if the shrinkage could be stopped, the heating rate was lowered to 1 K min^{-1}. This shifted the initiation point by approximately 70 K (to ~ 1700 K), but failed to stop the shrinkage. After this rapid compaction (point B in Fig. 3), the sample densified in a gradual fashion similar to the UBE powder, although the maximum density wasn't reached until 2023 K. In order to understand this phenomenon better, samples of the HPZ-derived powder were fired, under the same conditions, to temperatures corresponding to points A–C in Fig. 3. The resulting compacts were analysed by XRD, SEM, helium pycnometry and bulk density measurements. The XRD and SEM results are summarized in Figs 4 and 5, respectively. The following observations were made.

3.2.1. Point A

A sample of the HPZ-derived powder was fired to 1663 K and immediately cooled. The resultant compact was essentially amorphous by XRD with only minor (< 1–2 wt %) amounts of either α-Si_3N_4 or Y_2O_3 present (see curves a and b, Fig. 4). The bulk density of the sample was 1.19 g cm^{-3} and its specific gravity was 2.70 g cm^{-3}. Examination of a fracture surface by SEM showed that the morphology of the powder was unchanged from the starting powder (for comparison see Figs 1 and 5).

3.2.2. Point B

A sample of the HPZ-derived powder was heated at 1 K min^{-1} until the rapid LVDT movement was seen (~1700 K). At this point, the sample was immediately cooled. The resultant compact had a bulk density of 2.03 g cm^{-3} and a specific gravity of 3.24 g cm^{-3}. The higher specific gravity of the compact suggested that a phase change from amorphous to crystalline Si_3N_4 had occurred. This was confirmed by XRD analysis which showed that the sample was a 53/47 wt % mixture of crystalline α and β silicon nitride (see curve c, Fig. 4). An analysis of a fracture surface by SEM showed that the powder morphology was completely different. Instead of angular shards, the fracture surface consisted of a mixture of partially sintered, equiaxed particles with an average particle size of 0.1–0.3 μm embedded in a glassy phase (see Fig. 6).

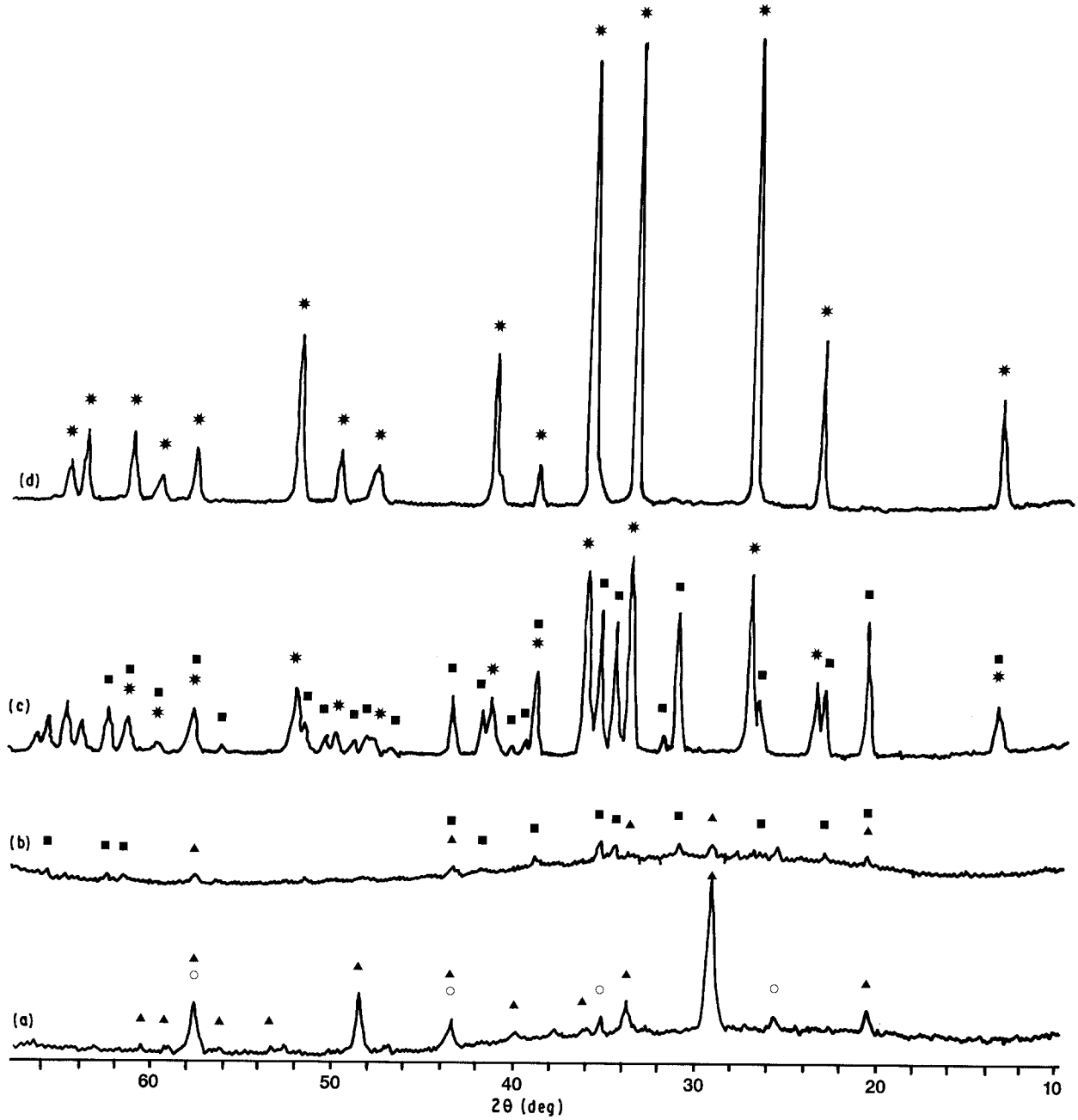

Figure 4 XRD diffractograms of a mixture of HPZ amorphous silicon nitride with 5 wt % Y_2O_3 and 3 wt % Al_2O_3: (a) before calcining; (b) after calcining to 1663 K with no hold (point A, Fig. 3); (c) after calcining to 1770 K with no hold (point B, Fig. 3); (d) after calcining at 2023 K for 90 min (point C, Fig. 3). Scale is for $2\theta = 60°$ to 70°. ▲, Y_2O_3; ○, Al_2O_3; ■, α-Si_3N_4; *, β-Si_3N_4.

Figure 5 Microstructure of a mixture of HPZ amorphous silicon nitride with 5 wt % Y_2O_3 and 3 wt % Al_2O_3 fired to 1663 K. SEM micrograph corresponds to point A in Fig. 3.

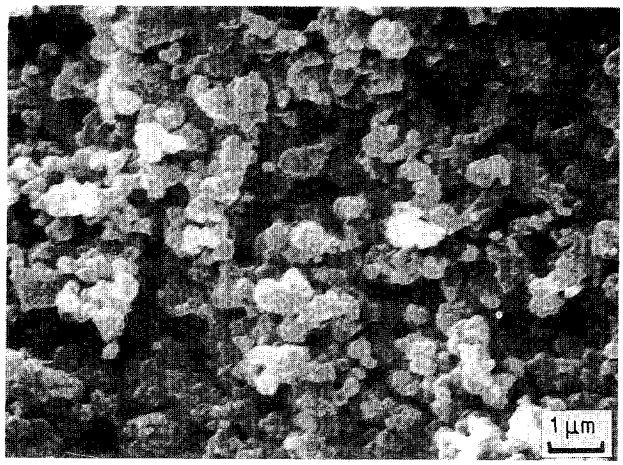

Figure 6 Microstructure of a mixture of HPZ amorphous silicon nitride with 5 wt % Y_2O_3 and 3 wt % Al_2O_3 fired to 1770 K. SEM micrograph corresponds to point B in Fig. 3.

The formation of an intermediate mixture of α- and β-Si_3N_4 crystallites is in stark contrast to the behaviour reported by Loehman and Rowcliffe [12] for a mixture of amorphous Si_3N_4 powders (GTE Sylvania SN 402) sintered with a mixture of Y_2O_3 and Al_2O_3 sintering aids. In their system, the amorphous portion of the SN 402 powder transformed directly to a β-Si_3N_4 without passing through an intermediate α phase.

3.2.3. Point C

After sintering at 2023 K for 90 min, the HPZ-derived Si_3N_4 compact had a bulk density of 3.23 $g\,cm^{-3}$. β-Si_3N_4 was the only crystalline phase observed by XRD (see curve d, Fig. 4).

3.3. DTA studies

A sample of the HPZ-derived Si_3N_4 powder, with and without sintering aids, was heated to 1723 K under nitrogen in a combination DTA/TGA cell. The amorphous powder without the Y_2O_3 and Al_2O_3 addition had a total weight loss of 11–12%. Mild exotherms were observed at 1335 and 1698 K. The transition at 1698 K was in good agreement with the amorphous-to-crystalline transitions reported by both Prochazka and Greskovich [5] and Yamada *et al.* [4]. Similar transitions were seen in the HPZ-derived powder with the Y_2O_3 and Al_2O_3 sintering aids. However, the transition which occurred at 1691 K was approximately four times more intense. In both cases, this transition occurs at the same point where the rapid LVDT movement was seen in the hot press run with a 1 K min^{-1} heating rate in our present study. Thus, our DTA/TGA data confirm that the rapid densification observed at ~1700 K is associated with the (α + β) transition of the amorphous Si_3N_4 powder.

After each DTA run, the residue was examined by SEM and compared wtih the microstructure of the compact from the corresponding hot-press run. In the absence of sintering aids, the DTA sample consisted of large, angular particles with an average particle size of approximately 1–2 μm and resembled the morphology of the initial HPZ Si_3N_4 powder. The morphology of the residue from the DTA run with the sintering aids present was equivalent to a compact fired to point B (see Fig. 6).

4. Conclusions

Clearly, under the influence of pressure and heat, HPZ- and PCS-derived amorphous silicon nitride powders doped with Y_2O_3 and Al_2O_3 sintering aids undergo a series of crystallographic, morphological and volume changes at approximately 1700 K. Prior to 1700 K, the powders retain their grain morphology and are amorphous by XRD. However, at ~1700 K a very rapid reaction between the Y_2O_3, Al_2O_3 and amorphous powder occurs. At this point, a glassy phase forms under pressure from which the α and β phases are nucleated. Evidence for the formation of a high-temperature glassy phase can be seen in Fig. 6. Both Prochazka [5] and Yamada *et al.* [4] have reported this transition as being very rapid and highly exothermic. Shortly after the glassy phase is generated, the viscosity of the system rapidly increases, either by dissipation of the localized heat or by the precipitation of the 0.1–0.3 μm α- and β-silicon nitride crystallites. At this point, the system is a mixture of small, equiaxed Si_3N_4 crystallites embedded in a glassy phase. Hence additional densification proceeds via typical sintering mechanisms. As a result, the microstructure, density and four-point MOR of the final piece is comparable to that obtained with a commercial, crystalline powder.

Acknowledgements

The authors would like to thank both Dan Petrak and Dan Filsinger of Dow Corning Corporation for their assistance in obtaining the hot-press and DTA data, respectively.

References

1. G. ZIEGLER, J. HEINRICH and G. WÖTTING, *J. Mater. Sci.* **22** (1987) 3041.
2. O. GLEMSER and P. NAUMANN, *J. Anorg. Allg. Chem.* **298** (1958) 134.
3. K. S. MAZDIYASNI and C. M. COOKE, *J. Amer. Ceram. Soc.* **56** (1973) 628.
4. T. YAMADA, T. KAWAHITO and T. IWAI, *J. Mater. Sci. Lett.* **2** (1983) 275.
5. S. PROCHAZKA and C. GRESKOVICH, *Amer. Ceram. Soc. Bull.* **57** (1978) 579.
6. T. YOSHIDA, T. TANI, H. NISHIMURA and K. AKASHI, *J. Appl. Phys.* **54** (1983) 640.
7. S. FUTAKI, Y. SHIMIZU, K. SHIRAISHI, Y. MORIYOSHI, T. SATO and T. SAKAI, *J. Mater. Sci.* **22** (1987) 4331.
8. W. X. PAN, M. SATO, T. YOSHIDA and K. AKASHI, *Adv. Ceram. Mater.* **3** (1988) 77.
9. W. R. CANNON, S. C. DANFORTH, J. H. FLINT, J. S. HAGGERTY and R. A. MARRA, *J. Amer. Ceram. Soc.* **65** (1982) 335.
10. H. T. SAWHILL and J.S. HAGGERTY, *ibid.* **65** (1982) C131.
11. G. T. BURNS and G. CHANDRA, *ibid.* **72** (1989) 333.
12. R. E. LOEHMAN and D. J. ROWCLIFFE, *ibid.* **63** (1980) 144.
13. M. SHIMADA, N. OGAWA, M. KOIZUMI, F. DACHILLE and R. ROY, *Amer. Ceram. Soc. Bull.* **58** (1979) 519.
14. S. YAJIMA, *ibid.* **62** (1983) 893.
15. G. E. LEGROW, T. F. LIM, J. LIPOWITZ and R. S. REAOCH, *ibid.* **66** (1987) 363.

Received 4 March
and accepted 1 July 1991